

HOW TO COUNT AND SIZE FLUORESCENT MICROBIAL PLANKTON WITH DIGITAL IMAGE FILTERING AND SEGMENTATION

Detlef Schröder, Christiane Krambeck and Hans-Jürgen Krambeck

Max-Planck-Institute of Limnology, Postfach 165, D-2320 Plön

ABSTRACT

A fast, reproducible, completely automatic and rather accurate way of quantitative determination of fluorescent microbial plankton is shown. In addition to the question about the organization of an image analyser, which should nearly work without any human intervention, some essential effects on enumeration and sizing of fluorescent cells are treated. Fine tuning between adjustment of the optical environment (camera intensity, dye concentration, focus level, magnification) and image interpretation algorithms as well as an object adapted application of image segmentation techniques (edge detection) are necessary. The edge detector should be able to separate adjacent objects on the basis of significant grey level distributions and changes within local image areas. Sources of error mainly caused by limited image resolution are made more transparent, whereby it is easier for the user to judge results of image analysis in epifluorescence microscopy.

KEYWORDS: bacterial biomass determination, epifluorescence microscopy, image filtering, image segmentation, SIT-video camera.

MOTIVATION AND SYSTEM ORGANIZATION

Seasonal variation in bacterial biomass plays an important part in the food web of the ecosystem "water". With the intention of monitoring growth and distribution of microbial plankton as continuous as possible, fast, accurate and reproducible evaluation methods are of interest. On the part of sample preparation staining bacterioplankton with fluorescent dye (DAPI or acridine orange) for counting and sizing cells with epifluorescence microscopy has become a favourite technique. But human direct counting does not sufficiently provide detailed quantitative and qualitative informations about a sample. Errors caused by fading and intuitive human sizing can be avoided by the application of computer supported image analysis systems. Video techniques advancing an increased automatic approach of image analysis has been developed during the last years (Fry, 1988, Sieracki et al., 1989, David and Paul, 1989, Krambeck et al., 1990, Schröder et al. 1990).

With the intention to speed up the daily routine of bacterial biomass determination the processes "microscoping" and "analysis" of sample pictures are separately executed. During microscoping the user randomly selects different sample fields (three to five

pictures with about 100 to 200 cells), focus level is adjusted, the picture is converted to a digital image with 512 x 640 square and grey-scaled (0=black..255=white) pixels in real-time. The images are stored on hard disks or optical disks within a sample description file structure. The later analysis of all stored images by a batch program do not require the user's presence.

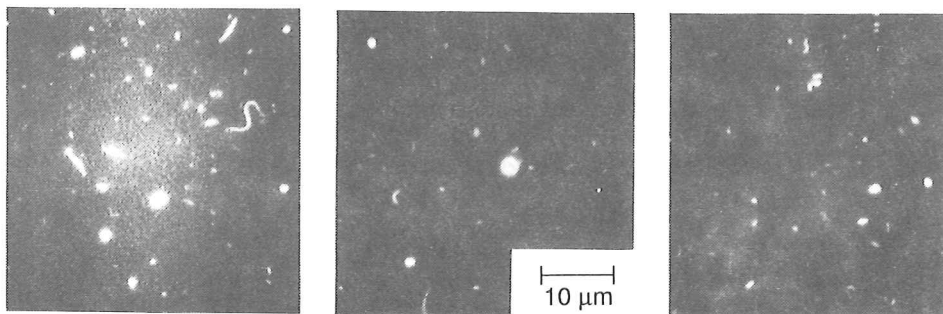


Figure 1. Digitized fluorescent bacterioplankton stained by three different DAPI concentrations (from left to right: 1.3 µg/l, 5.1 µg/l, 10.2 µg/l).

PRECONDITIONS

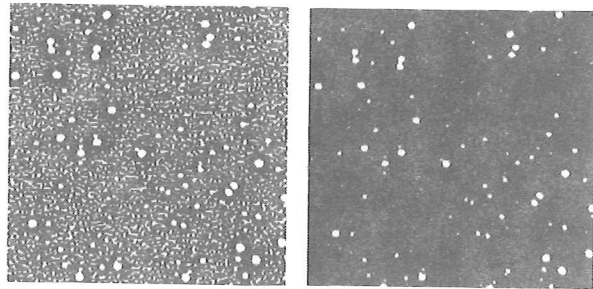
Optimal sample preparation is the basic precondition for correct cell detection and sizing. It is important to adapt staining intensity to the light sensitivity of the image recording system. We use a silicon-intensified target (SIT)-video camera, which is necessary for the detection of small bacteria near the resolution limit of epifluorescence microscopy ($<0.3 \mu\text{m}$). Even this extremely light sensitive SIT-camera is not able to make small bacteria visible, if the concentration of dye is too low (1.3 µg DAPI/l) (Figure 1, left). Amplification of the video signal induces distinct background noise. Otherwise, if too much dye is used (10.2 µg DAPI/l) (Figure 1, right) fluorescent cells overshine, the background becomes discoloured and superfluous cloudy detritus is created. Stable results with respect to number and biovolume of natural bacterioplankton, which was stained by different dye concentrations (arranged in equidistant grades), were achieved in a range round 5.1 µg DAPI/ml (Figure 1, middle). Staining intensity depends on camera sensitivity and microscope objective characteristics. Magnification is the most crucial limitation factor in epifluorescence microscopy. On the one hand a magnification factor of more than 2000 does not make sense - it would only be an empty magnification -, but on the other hand accuracy in sizing small cells requires as many pixel as possible. The length of a single pixel corresponds to $0.089 \mu\text{m}$ at a 2000fold magnification, and the length of many aquatic bacteria amounts $0.4 \mu\text{m}$ to $0.8 \mu\text{m}$. Thus it can not be dispensed with a pixel. Adjustment of the correct focus level is the third and last precondition for successful cell detection and sizing. Effects of variation in focus level will be considered later.

OBJECT ADAPTED IMAGE SEGMENTATION

Before a digital image can be binary segmented into disjunct sets of background resp. object pixels, answers to following questions should be found: which image regions do form objects? Which typical brightness distribution (pattern) do they possess? Is it

possible to describe definitely these object characteristics by algorithms? Which image segmentation method does take the digital object description into account? In other words image segmentation methods are adapted to visual object characteristics.

Bacterioplankton can be described as "image regions with an interior homogeneous grey value distribution (called plateau) and a continuously weakly increasing resp. decreasing transition zone (called edge) between darker background and brighter cell center". Short frequent changes in grey level reflects e.g. noise in the background caused by amplification (Figure 1, left).



10 μm

Figure 2. Failed binary segmentation of fluorescent objects by thresholds of 235 (left) resp. 250 (right).

Since object "plateaus" are found on different grey levels, the absolute grey value of a pixel is not an indicator for its membership of object image regions. For this reason thresholding is not a suitable image segmentation method in this application. Figure 2 demonstrates, that it is impossible to find a fit threshold in a digital image of fluorescent objects. Small variation in thresholding induces strong differences in segmentation results concerning number and size of objects.

Gradient segmentation methods consider increases and decreases of pixel brightness within an local image area. Edges (=transition zones between object and background) can be detected by gradient operators.

A gradient segmentation method works with well balanced quadratic arrays of symmetric arranged weights (sum of weights = 0) called filter kernels (Figure 3).

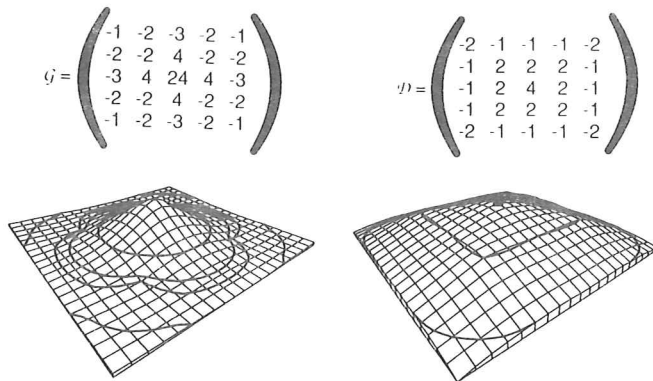


Figure 3. Gradient filter kernels "Mexican Hat" (G) (left) and own design (D) (right).

In the scope of filtering an digital image I, each pixel I(x,y) is replaced by a weighted sum of its neighbours:

$$I'(x,y) = \sum_{k=-2}^2 \sum_{l=-2}^2 (I(x+k,y+l) * D(k,l)). \quad (1)$$

Image filtering by (1) results in a gradient image (second derivative of the original image). Marr and Hildreth (1980), Haberäcker (1985), Smith et al. (1988) give a detailed view into the theory of gradient operators. Arrangement and composition of the filter kernel decide success or failure in edge detection. Some familiar operators like the Laplacian amplify frequency noise in fluorescence images. This leads to misinterpretations, "real" edges are not obviously distinguishable from noise. Smoothing noisy images during edge detection avoids these problems. Application of Marr and Hildreth's "Mexican Hat" G as well as our filter kernel D (Figure 3), which is not as noise-sensitive as kernel G, causes a smoothed center of a local image environment and an accentuation of grey level differences between margin and center. The filter kernel's dimension depends on the range, which is considered to be noise or a small object. In consideration of tiny aquatic bacteria dimension 5 is advisable. Characteristics of gradient images produced by our gradient operator as well as effects on edge detection and cell sizing by image filtering were examined on the basis of a microspherical edge model. Supposing that edge characteristics (edge profiles) of fluorescent latex beads (Figure 4) are similar to those of natural bacteria cells, accuracy in computing cell boundaries (contours) subsequent to image filtering can be scrutinized by means of the microsphere model.

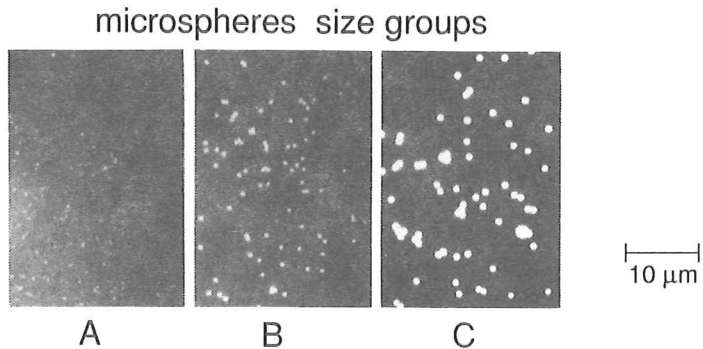


Figure 4. Fluorescent latex beads of different sizes (A=0.27 μm , B=0.58 μm , C=0.88 μm) used as microspherical edge model.

Figure 5c shows profiles over a digital image part (Figure 5a) and its corresponding part of the gradient image (Figure 5b). The gradient curve reacts on changes in the slope intensity of the original image profile with a 5-pixel-environment (depending on filter kernel dimension). Negative gradient curve indicates increasing original profile and vice versa. Therefore edges (positive peaks at the object marginal zones) are surrounded by distinct negative peaks ("valleys"). Positive peaks overlap, if the homogeneous object plateau between the edges is covered by the filter kernel. An intersection cross the gradient image results in edges (above the gradient intersection threshold level) and background resp. object interiors (below the threshold).

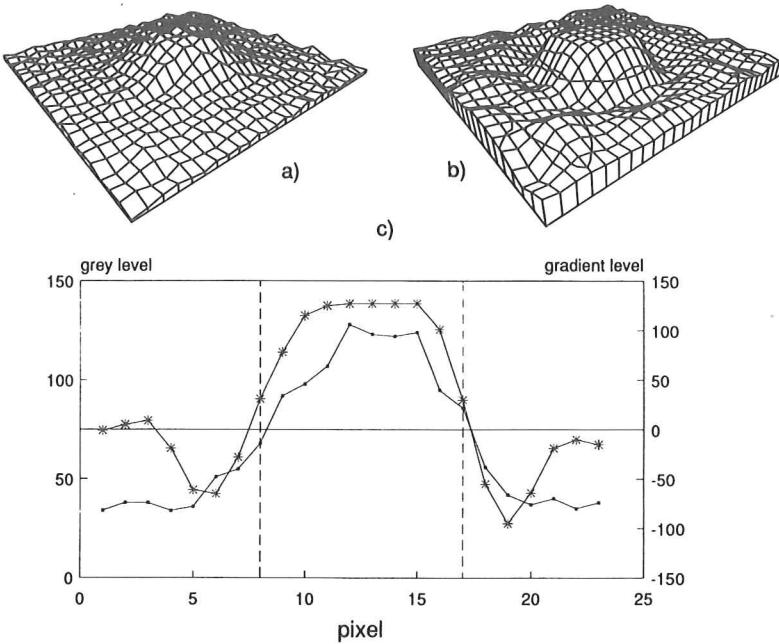


Figure 5. Fluorescent latex bead within original digital image (a) and gradient image (b). Below: profiles over original (____) and gradient image (-*-); "real" microsphere boundary (----).

ACCURACY

Although weak and continuous increases and decreases of grey level changes in a digital image are marked and recognizable, one question remains; which intensity of increase or decrease, that means which gradient level does indicate "real" object boundary points? Calibration against fluorescent objects of known size is necessary. Size distribution and mean diameter of three groups of latex beads were determined by scanning electron microscopy (SEM) (Figure 6) and give a clue to results of sizing the same microspheres by epifluorescence microscopy (digital filtering and subsequent edge detection described above). Small-scaled variation in gradient threshold (80 to 120) does not influence results of sizing in a high degree; they remain nearly stable. Figure 6 shows size distribution computed after an intersection of the gradient image at a level of 100. The three size classes are obviously noticeable. The larger dispersion in every size class (width of the size classes) as well as small overlaps are due to several reasons. The rough pixel grid caused by limited image resolution is the main one. Real microsphere sizes are not a multiple of the pixel length. Furthermore fragments of beads, destroyed during preparation, blurred marginal zones of the

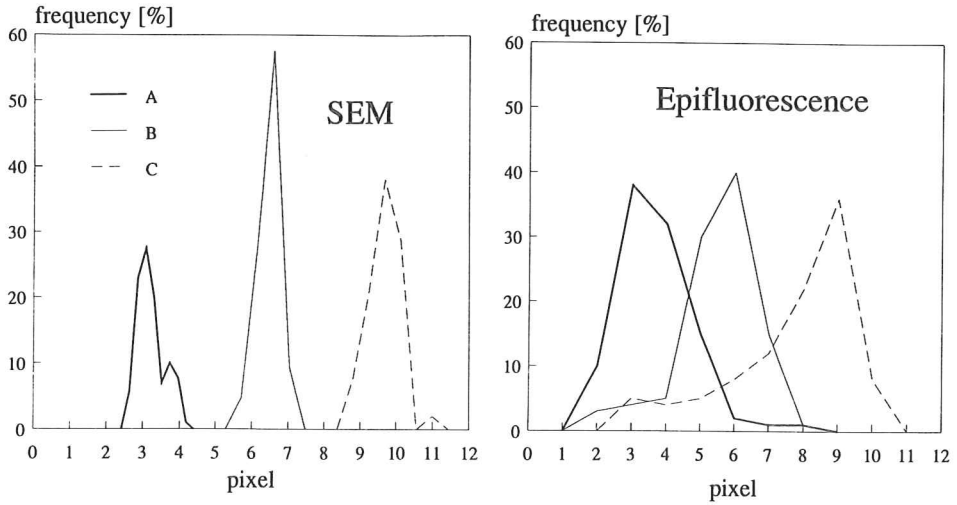


Figure 6. Size distribution of latex beads determined by scanning electron microscopy (SEM) and digital segmentation in epifluorescence microscopy.

objective as well as unseparated adjacent microspheres have an effect on size distribution determination.

Evaluation of mixed bead samples containing all kinds of microspheres illustrates the problem of focus level adjustment. Focus on size C induces lost of small microspheres (Figure 7). Vice versa, if small beads (size A) are in focus, big beads appear a little bit smaller (their peak in the size distribution curve extends to 9 and 10 pixels). That is the reason why automatic plankton enumeration and sizing at our institute is restricted for the present to cells with a length under one micrometer. How to handle mixed samples (cells of different sizes and structures) will be the next job.

During microscoping small cells logically has to be in focus in order to count all cells. Separation of adjacent objects is a particular delicate problem in image analysis. This

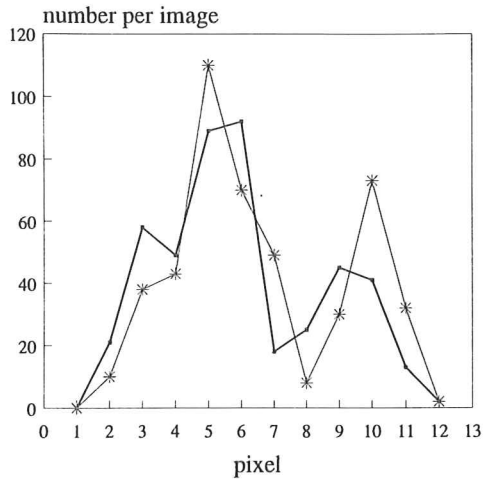


Figure 7. Effects on sizing by focus variation. Beads of size A in focus (—) resp. beads of size C in focus (-*-).

problem is tackled by taking advantage of one useful characteristic of our gradient operator. Local changes in the trend of an edge profile curve are indicated by negative peaks in the gradient curve. Figure 8 demonstrates this effect. Original and gradient profiles over two adjacent microspheres (the left one is of size C and the right of size A) are displayed. Overlapping descendent edge profile of the big and bright microsphere and the ascending edge profile of the small and dark bead cause an interrupt in the profile curve trend reflected by a negative peak in the gradient image. Since this peak is below gradient threshold an intersection cross the gradient image results in a successful separation of the adjacent microspheres.

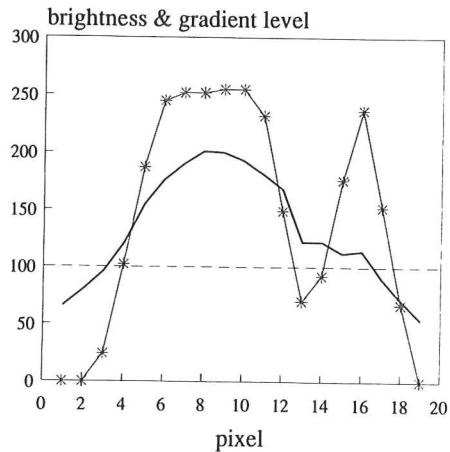


Figure 8. Profiles over original (—) and gradient image (-*-) part with two adjacent microspheres of size A (right) and size C (left), which can be separated.

ACKNOWLEDGEMENT

We thank the "Deutsche Forschungsgemeinschaft", who supports our project titled (DFG II B1-Kr971/1-1 "Limnologische Bildanalyse".

REFERENCES

- David AW, Paul, JH. Enumeration and sizing of aquatic bacteria by use of a silicon-intensified target camera linked - image analysis system. *J Microbiol Methods*, 1989; 9: 257-266.
- Fry DC. Determination of Biomass. In: Austin B, ed. *Methods in Aquatic Bacteriology*. John Wiley & Sons Ltd., 1985: 27-72.
- Haberäcker P. *Digitale Bildverarbeitung*. Wien: Hanser Verlag, 1985.
- Krambeck C, Krambeck HJ, Schröder D, Newell SY. Sizing bacterioplankton: a Juxtaposition of Bias due to Shrinkage, Halos, Subjectivity in Image Interpretation and Asymmetric Distributions. *Binary Comp in Microbiol*, 1990; 2: 11-20.
- Marr D, Hildreth E. Theory of edge detection. *Proc. R. Soc. Lond.*, 1980; 207: 187-217.
- Schröder D, Krambeck HJ. Advances in digital image analysis of bacterioplankton with epifluorescence microscopy. *Verh. Int. Verein. Limnol.*, 1990: in press.
- Sieracki M, Reichenbach S, Webb K. Evaluation of Automated Threshold Selection Methods for Accurately Sizing Microscopic Fluorescent Cells by Image Analysis. *Applied and Environmental Microbiology*, 1989; 55: 2762-2772.
- Smith T, Marks W, Lange G, Sherief W, Neale E. Edge detection in images using Marr-Hildreth filtering techniques. *J Neuroscience Methods*, 1988; 26: 75-82.

Presented at the 7WQIA in Freiburg 90.